HHS Public Access

Author manuscript

J Biomater Sci Polym Ed. Author manuscript; available in PMC 2015 July 28.

Published in final edited form as:

J Biomater Sci Polym Ed. 2014 ; 25(13): 1387–1406. doi:10.1080/09205063.2014.940243.

Carbohydrate-functionalized nanovaccines preserve HIV-1 antigen stability and activate antigen presenting cells

J.E. Vela Ramirez[1], **R. Roychoudhury**[2], **H.H. Habte**[3,4,¶], **M. W. Cho**[3,4,†], **N. L. B. Pohl**[2], and **B. Narasimhan**[1,*]

[1]Department of Chemical and Biological Engineering, Iowa State University, Ames, IA 50011

[2]Department of Chemistry, Indiana University, Bloomington, IN 47405

[3]Department of Biomedical Sciences, Iowa State University, Ames, IA 50011

[4]Center for Advanced Host Defenses, Immunobiotics and Translational Comparative Medicine, Iowa State University, Ames, IA 50011

Abstract

The functionalization of polymeric nanoparticles with ligands that target specific receptors on immune cells offers the opportunity to tailor adjuvant properties by conferring pathogen mimicking attributes to the particles. Polyanhydride nanoparticles are promising vaccine adjuvants with desirable characteristics such as immunomodulation, sustained antigen release, activation of antigen presenting cells, and stabilization of protein antigens. These capabilities can be exploited to design nanovaccines against viral pathogens, such as HIV-1, due to the important role of dendritic cells and macrophages in viral spread. In this work, an optimized process was developed for carbohydrate functionalization of HIV-1 antigen-loaded polyanhydride nanoparticles. The carbohydrate-functionalized nanoparticles preserved antigenic properties upon release and also enabled sustained antigen release kinetics. Particle internalization was observed to be chemistry-dependent with positively charged nanoparticles being taken up more efficiently by dendritic cells. Up-regulation of the activation makers CD40 and CD206 was demonstrated with carboxymethyl-α-D-mannopyranosyl-(1,2)-D-mannopyranoside functionalized nanoparticles. The secretion of the cytokines IL-6 and TNF-α was shown to be chemistry-dependent upon stimulation with carbohydrate-functionalized nanoparticles. These results offer important new insights upon the interactions between carbohydrate-functionalized nanoparticles and antigen presenting cells and provide foundational information for the rational design of targeted nanovaccines against HIV-1.

Keywords

dendritic cells; carbohydrates; nanoparticles; polyanhydrides; targeting; HIV antigen; nanovaccines

*To whom all correspondence should be addressed, Phone: 515-294-8019; nbalaji@iastate.edu.

¶Current address: Boehringer Ingelheim, Department of Biotherapeutics, Ridgefield, CT 06877

†Requests for pET-gp41-54Q-GHC should be made to MWC (mcho@iastate.edu).

Introduction

Functionalization of antigen delivery platforms to enable active targeting of cells is a well-studied approach for the design of novel adjuvants/delivery formulations for vaccines [1–4]. Activation of cellular receptors on antigen presenting cells (APCs) can enable tailored immune responses against pathogens [5–7]. One such approach is the use of carbohydrate moieties to activate pattern recognition receptors like C-type lectin receptors (CLRs), which play an important role in both innate and adaptive immune responses [2,5,8–11]. This strategy could be important for viral infections, particularly human immunodeficiency virus (HIV), due to the key role of dendritic cells (DCs) and macrophages in the spread of the virus [12–15].

In recent years the HIV epidemic has become one of the greatest challenges for researchers around the world [16–17]. Since its outbreak in 1981, more than 25 million people have died of Acquired Immunodeficiency Syndrome (AIDS), and over 33 million people are currently infected [18]. HIV-1 infection is characterized by the inhibition of the immune response from $CD4^+$ T cells that allows constant replication of the virus and depletion of T helper cells, which ultimately causes disease progression [12,16,19–21]. One of the mechanisms that HIV-1 uses to block the immune response due to $CD4^+$ T cells is infection of plasmacytoid DCs to prevent the maturation and proliferation of these cells, resulting in the induction of a T regulatory lineage [12,14,15,22–24]. Given the multiple roles that DCs play in the innate and adaptive immune responses, other functions are also affected due to the interaction of the virus with these cells. These include suppression of TLR7 and TLR9 activation, which are known antiviral Toll-like receptors, and blockage of the release of Type I and II interferons [15, 22]. Therefore, it has been hypothesized that activation of DCs is required to prevent HIV-1 infection [7,15,22].

One of the main strategies to prevent the continuous spread of HIV-1 worldwide is the development of an efficacious vaccine [16,19,25]. Presently, one of the main foci in the development of efficacious HIV-1 vaccines is the use of recombinant proteins as antigens [16,17,26]. Even though these antigens are safe, they are poorly immunogenic, and therefore need an adjuvant to elicit a robust immune response [26]. In this regard, biodegradable polyanhydride nanoparticles have shown promise as adjuvants and/or delivery vehicles with beneficial properties, including antigen stabilization, sustained antigen release, APC activation, and immune modulation, that can be exploited to formulate a successful HIV-1 vaccine [27–34]. This study focuses on the use of gp41-54Q–GHC as the immunogen (to be described in more detail elsewhere), which contains the Heptad Repeat Region 2 (HR2) and the membrane proximal external region (MPER) of the HIV-1 glycoprotein gp41 [26]. Polyanhydride nanoparticles based on sebacic acid (SA) 1,6-bis(p-carboxyphenoxy) hexane (CPH), and 1,8-bis(p-carboxyphenoxy)-3,6-dioxaoctane (CPTEG) and CPH were used to encapsulate and release stable gp41-54Q–GHC immunogen. The nanoparticles were functionalized with carboxymethyl-α-D-mannopyranosyl-(1,2)-D-mannopyranoside (di-mannose) to specifically target the macrophage mannose receptor (MMR). Bone marrow derived DCs were stimulated with these nanoparticles and their activation patterns were analyzed. The current studies demonstrate the dual capabilities of functionalized polyanhydride nanoparticles to stabilize an HIV-1 antigen and to target and activate DCs.

Materials and Methods

Materials

Chemicals needed for monomer synthesis, polymerization, and nanoparticle synthesis included 1-methyl-2-pyrrolidinone, anhydrous (99+%), terephthalic acid (99+%) and sebacic acid (99%) and all were purchased from Aldrich (Milwaukee, WI); 1,6-dibromohexane, 4-*p*-hydroxybenzoic acid, and triethylene glycol were purchased from Sigma Aldrich (St. Louis, MO); 4-*p*-fluorobenzonitrile was obtained from Apollo Scientific (Cheshire, UK); acetic acid, acetic anhydride, acetonitrile, dimethyl formamide (DMF), ethyl ether, hexane, methylene chloride, pentane, petroleum ether, potassium carbonate, sulfuric acid, and toluene were purchased from Fisher Scientific (Fairlawn, NJ). For NMR characterization, deuterated chemicals, including chloroform and dimethyl sulfoxide (DMSO), were purchased from Cambridge Isotope Laboratories (Andover, MA). For nanoparticle functionalization, 1-ethyl-3-(3-dimethylaminopropyl) carbodiimide hydrochloride, *N*-hydroxysuccinimide, and ethylenediamine were purchased from Thermo Scientific (Waltham, MA). Glycolic acid was purchased from Acros Organics (Pittsburgh, PA). β-Mercaptoethanol, *Escherichia coli* lipopolysaccharide (LPS) O26:B6, and rat immunoglobulin (rat IgG) were purchased from Sigma Aldrich (St. Louis, MO). Materials required for the DC culture medium included: granulocyte-macrophage colony-stimulating factor (GM-CSF), purchased from PeproTech (Rocky Hill, NJ); HEPES buffer, RPMI 1640, penicillin-streptomycin, and L-glutamine, purchased from Mediatech (Herndon, VA); and heat inactivated fetal bovine serum, purchased from Atlanta Biologicals (Atlanta, GA). Materials used for flow cytometry included: BD stabilizing fixative solution purchased from BD Bioscience (San Jose, CA); unlabeled anti-CD16/32 FcγR, purchased from Southern Biotech (Birmingham, AL); allophycocyanin (APC) anti-mouse CD40 (clone 1C10), Alexa Fluor® 700 conjugated anti-mouse MHC Class II (I-A/I-E) (clone M5/114.15.2) and their corresponding isotypes APC-conjugated rat IgG2aκ (clone eBR2a), PE-conjugated rat IgG2aκ (clone eBR2a), Alexa Fluor 700®-conjugated rat IgG2bκ were purchased from eBiosciences (San Diego, CA). APC/Cy7 conjugated anti-mouse CD11c (clone N418), PE/Cy7 conjugated anti-mouse CD86 (clone GL-1), FITC conjugated anti-mouse CD206 (clone C068C2) and their corresponding isotypes APC/Cy7 conjugated Armenian Hamster IgG (clone HTK888), PE/Cy7 conjugated rat IgG2aκ (clone RTK2758), FITC conjugated rat IgG2aκ (clone RTK2758) were purchased from BioLegend (San Diego, CA). Cadmium selenide quantum dots (QDs) (emission at 630 nm) were a kind gift from Dr. Aaron Clapp at Iowa State University.

Construction of pET-gp41-54Q–GHC

The plasmid encoding gp41-54Q–GHC was constructed based on pET-gp41-54Q (to be described elsewhere), which encodes 54 amino acids of the C-terminal ectodomain of HIV-1 gp41 (based on M group consensus sequence, MCON6). The terminal lysine residue was mutated to glutamine. A short linker (GSGSG), followed by a 6xHis tag and a cysteine residue (C) was attached right after the Gln (Q) by PCR using a forward primer 5’-CGCGGATCCGAGTGGGAGCGCGAGATC-3’ and a reverse primer 5’-CCATGAATTCTTAGCAATGGTGATGATGGTGATGTCCCGATCCCGATCCC TGGATGTACCACAGCCAGTT-3’. The PCR product was digested by BamHI and EcoRI

and then ligated into corresponding sites in pET-21a to yield pET-gp41-54Q–GHC. Construct was confirmed by sequencing.

Expression and purification of gp41-54Q-GHC

Protein expression and purification were performed according to the method of Penn-Nicholson et al. [35] with a few modifications. For gp41-54Q–GHC expression, *E. coli* T7 Express IysY/Iq (New England Biolabs) was transformed with pET-gp41-54Q–GHC and cultured overnight at 37 °C in superbroth containing ampicillin (50 μg/mL). Cells were diluted 1:100 in fresh superbroth and cultured to 1.0 OD_{600} at 37°C. Protein expression was then induced with 1 mM isopropyl-beta-D-thiogalactopyranoside (IPTG) and continued to grow until OD_{600} reached 5.0. Cells were harvested by centrifugation at 4,600 rcf for 30 min in a Sorvall Legend XFR centrifuge (Thermo Scientific). The cell pellet was washed in phosphate-buffered saline (PBS, pH 7.4) and lysed by sonication using a Branson Digital Sonifier. The sample was sonicated until the suspension became translucent, followed by centrifugation at 15,000 rcf for 20 min in Avanti® J-26 XPI centrifuge (Beckman Coulter). After an additional three repetitions of PBS resuspension, sonication, and centrifugation, the pellet containing inclusion bodies was solubilized in PBS containing 8 M urea and sonicated. Insoluble debris was removed by centrifugation at 15,000 rcf for 20 min, and soluble proteins were bound to Ni-NTA resin (QIAGEN) by mixing on an end to end shaker overnight at 4 °C. The mixture was loaded onto a column, and the protein was renatured through serial incubations with 20 bed volumes of PBS containing a decreasing step gradient of urea at 8 M, 6 M, 4 M, 3 M, 2 M, 1 M, and 0 M. The column was washed with PBS containing 20 mM imidazole, and the protein was eluted with PBS containing 250 mM of imidazole. Purified protein was finally dialyzed in PBS (pH 8). The endotoxin content in gp41-54Q–GHC was quantified using a commercially available QCL-1000 Limulus Amebocyte Lysate (LAL) kit (Lonza, Switzerland) and found to be <0.1pg/μg of protein, which is acceptable for use in cell-based assays [36–38] for subunit proteins.

Monomer and polymer synthesis

Monomers of 1,6-bis(*p*-carboxyphenoxy) hexane (CPH) and 1,8-bis(*p*-carboxyphenoxy)-3,6-dioxaoctane (CPTEG) were synthesized as described previously [27,29,39]. CPTEG:CPH and CPH: SA copolymers of various ratios were synthesized by melt polycondensation as previously described [39–41]. The chemical structure was characterized with ^1H NMR using a Varian VXR 300 MHz spectrometer (Varian Inc., Palo Alto, CA) and the molecular mass was determined using gel permeation chromatography (GPC) on a Waters GPC chromatograph (Milford, MA) containing PL gel columns (Polymer Laboratories, Amherst, MA). The synthesized 50:50 CPTEG:CPH copolymer had a M_w of 5,400 Da, the 20:80 CPH:SA copolymer had a M_w of 14,400 Da and the 20:80 CPTEG:CPH copolymer had a M_w of 7,700 Da. The polydispersity indexes (PDI) of these copolymers were 1.5, 1.4 and 1.3, respectively. These values are consistent with previous work [29–33,39].

Nanoparticle synthesis

Polyanhydride nanoparticles were synthesized using anti-solvent nanoencapsulation as described previously [42]. Briefly, gp41-54Q–GHC (1% w/w) and 20 mg/mL polymer were dissolved in methylene chloride (at 4°C for 50:50 CPTEG:CPH and at room temperature (RT) for 20:80 CPH:SA). The polymer solution was sonicated at 40 Hz for 30 s using a probe sonicator (Ultra Sonic Processor VC 130PB, Sonics Vibra Cell, Newtown, CT) to create a homogeneous protein/polymer mixture and rapidly poured into a pentane bath (at −40°C for CPTEG:CPH and at RT for CPH:SA) at a solvent to non-solvent ratio of 1:250. Particles were then collected by filtration and dried under vacuum for 1 h.

Nanoparticle functionalization

Synthesis of carboxylated di-mannose—carboxymethyl-α-D-mannopyranosyl-(1,2)-D-mannopyranoside was synthesized using an alkenyl fluorous tag as previously reported [43]. Fluorous solid phase extraction (FSPE) was used to purify all the intermediates [44–46]. The double bond was cleaved by ozonolysis to produce an aldehyde at the reducing end, which was further oxidized to carboxylic acid by Jones oxidation. The global deprotection of the protecting groups was carried out by Birch reduction to generate the target dimannoside [47–50].

Surface functionalization—carboxymethyl-α-D-mannopyranosyl-(1,2)-D-mannopyranoside was conjugated onto the surface of polyanhydride nanoparticles using an amine-carboxylic acid coupling reaction [47–50]. Particles with glycolic acid groups on the surface (linker) and non-functionalized (NF) particles were used as controls. The conjugation reaction was performed in two reaction steps. Briefly, a nanoparticle suspension was made in nanopure water (10 mg/mL), and 10 equivalents of 1-ethyl-3-(3-dimethylaminopropyl)-carbodiimide hydrochloride (EDC) and 12 equivalents of *N*-hydroxysuccinimide (NHS), and 10 equivalents of ethylenediamine were added. This reaction was carried out at 4°C temperature for 1 h at a constant agitation of 17 rcf. Following the reaction, the particles were centrifuged at 10,000 rcf for 10 min and the supernatant was removed. The particles were washed with the same volume of nanopure water, centrifuged at 10,000 rcf for 10 min and the supernatant was removed. A second reaction was performed with 10 eq. of EDC, 12 eq. of NHS and 10 eq. of the corresponding functionalizing agent (i.e., di-mannose or glycolic acid) in nanopure water, using constant agitation at 17 rcf for 1 h at 4°C. Particles were sonicated before and after each reaction to break aggregates. After the reaction was completed, nanoparticles were collected by centrifugation (10,000 rcf, 10 min) and dried under vacuum for 1 h.

Nanoparticle characterization

Characterization of morphology and size of both the functionalized and the NF nanoparticles was performed using scanning electron microscopy (SEM, FEI Quanta 250, Kyoto, Japan) and quasi-elastic light scattering (QELS, Zetasizer Nano, Malvern Instruments Ltd., Worchester, UK). In order to confirm the successful attachment of the glycans onto the nanoparticles, QELS was used to measure the ζ-potential of the nanoparticles. To quantify the amounts of the carbohydrates conjugated to the nanoparticles, a high throughput version

of a phenol-sulfuric acid assay was used [47,51]. A microplate reader (SpectraMax M3, Molecular Devices, Sunnyvale, CA) was used to obtain the absorbance of standards and unknown samples using a wavelength of 490 nm. The total amount of sugar per unit weight of nanoparticles (μg/mg) was calculated.

Antigen release kinetics

In vitro antigen release kinetics studies were performed using a micro bicinchoninic acid (BCA) assay. Samples of protein-loaded nanoparticles were suspended in 750 μL of phosphate buffered saline (0.1 M, pH 7.4) with 0.01% w/v sodium azide and incubated at 37°C and 106 rcf. For each time point, samples were centrifuged at 10,000 rcf for 10 min, the supernatant was removed and aliquoted at 4°C, and fresh buffer was added to each sample to maintain perfect sink conditions. Aliquots were analyzed using micro BCA at an absorbance of 562 nm. Ethylenediamine-functionalized nanoparticles were used as a control for carbohydrate-modified nanoparticle quantification because the ethylene glycol linker interfered with the micro BCA assay. The experiment was carried out for 30 days, and the amount of released protein was normalized with total amount of protein encapsulated, as described previously [52,53]. After 30 days, the remaining protein was extracted by adding 750 μL of 17 mM NaOH solution. Protein encapsulation efficiency and antigen loss because of functionalization conditions were estimated using the micro-BCA assay.

Gel electrophoresis

For electrophoretic analysis of released gp41-54Q–GHC, nanoparticles were suspended in 250 μL of PBS (pH 7.4) for 1 h. After incubation, samples were centrifuged at 10,000 rcf for 10 min and supernatants were removed and stored for further analysis. Protein concentrations were measured using a micro-BCA assay and 500 ng of gp41-54Q–GHC released from each polymer chemistry was loaded in 4–20% polyacrylamide gels and run for 2 h at 120 V. Protein standards (10–250 kDa) were used to measure molecular weight. The gels were incubated in fixative solution (40% methanol, 10% acetic acid) for 3 h at 4°C. Staining with Flamingo fluorescent gel stain (BioRad Laboratories, Richmond, CA) was performed at 4°C overnight. Gels were scanned using a Typhoon 9410 Variable Mode Imager (GE Healthcare) [54].

Antigenic analysis of released immunogen

Antigenic analysis of gp41-54Q–GHC immunogen one hour after release from NF and functionalized 50:50 CPTEG:CPH nanoparticles was performed using an enzyme-linked immunosorbent assay (ELISA). Briefly, gp41-54Q–GHC (30 ng/well) was coated onto 96 well Costar™ High Binding plates (Costar #3590) using antigen coating buffer (15 mM Na_2CO_3, 35 mM $NaHCO_3$, 3 mM NaN_3, pH 9.6) overnight at 4°C. Non-specific antibody binding was prevented by blocking wells with 290 μL of PBS (pH 7.4) containing 2.5% skim milk and 10% fetal bovine serum (FBS) (1 h at 37°C). Plates were washed six times with 0.1% Tween 20 in PBS. Primary antibodies (2F5 [55–57], 4E10 [58] and Z13e1 [59–60]) were diluted at 1:1,000 in blocking buffer, and 100 μl were added to each well and incubated for 2 h at 37°C. The plates were washed six times and secondary antibody (goat anti-human) (Thermo-Scientific; Cat# 31430) at 1:3,000 dilution was added to each well and

incubated (100 μL, 1 h at 37°C). The plate washing process was repeated six times and wells were developed using 100 μL of TMB-HRP substrate for 10 min. The reaction was stopped with 50 μL of 2 N H_2SO_4. The developed plates were analyzed using a microplate reader (SpectraMax M3).

In vitro DC uptake and activation

Mice—C57BL/6 (B6) mice were purchased from Harlan Laboratories (Indianapolis, IN). Mice were housed in specific pathogen-free conditions where all bedding, caging, and feed were sterilized prior to use. All animal procedures were conducted with the approval of the Iowa State University Institutional Animal Care and Use Committee.

DC culture and stimulation—Dendritic cells were derived from bone marrow, harvested from tibias and femurs of C57/BL6 mice as described previously in published protocols [40, 47, 50,61]. DCs were >90% positive for CD11c (data not shown). Briefly, mice were euthanized using carbon dioxide inhalation and cardiac puncture was performed to ensure death. Bone marrow cells were harvested from tibias and femurs, and cultured in 10 mL of DC media containing RPMI-1640 with 10% FBS, 5% penicillin/streptomycin, 5% 2mM L-glutamine, 0.5% gentamycin, 2.5% HEPES buffer, 0.1% β-mercaptoethanol, and 0.1% granulocyte macrophage colony-stimulating factor (GMCSF) in T-75 cell culture grade flasks. At day 2, 10 mL of fresh DC media was added. At day 6, 10 mL of DC media were removed, centrifuged at 250 rcf for 10 min, and cells were resuspended in fresh media and added to corresponding flasks. At day 8, DCs were removed from the flasks, centrifuged at 250 rcf for 10 min and counted for plating. Cells were plated in 24 well plates using a concentration of 1×10^6 cells per well. GMCSF was added at 0.1 vol.% to DC media on days 0, 2, and 6. The DCs were stimulated with 200 ng/mL of *Escherichia coli* lipopolysaccharide (LPS, positive control) or polyanhydride nanoparticles at 125 μg/mL [40,42,45–50]. Non-stimulated (NS) cells were used as a negative control [40,42].

Particle internalization—Analysis of particle internalization was performed by co-encapsulating quantum dots (QDs, 630 nm emission) and gp41-54Q-GHC. 1% (w/w) QD-loaded and 1% (w/w) gp41-54Q-GHC-loaded polyanhydride nanoparticles were prepared. Nanoparticles were suspended in PBS for 48 h and supernatants were collected and used to stimulate DCs as a control to account for released QDs [61,62]. Bone marrow-derived DCs were stimulated with nanoparticle formulations for 48 h and using flow cytometry, particle positive cells were quantified. Non-stimulated cells were used as control [61,62].

Flow cytometric analysis of cell surface markers and CLRs—Cultured cells were analyzed using flow cytometry as described previously [40–42]. Antibodies for CD40, CD86, MHC II and CD206 and their corresponding isotypes were used in these studies. Samples were analyzed using a Becton-Dickinson FACSCanto™ flow cytometer (San Jose, CA) and the data was processed using the FlowJo vX software (TreeStar Inc., Ashland, OR).

Cytokine secretion

Supernatants of cultured cells were recovered 48 h post-stimulation and were analyzed for presence of IL-6, IL1-β, TNF-α, IL-12p40, and IFN-γ using a multiplex cytokine assay

processed in a Bio-Plex 200 ™ system (Bio-Rad, Hercules, CA) as described in previous protocols [40,52].

Statistical analysis

The cell surface marker expression and cytokine secretion data were subjected to statistical analysis using Prism6 (GraphPad, La Jolla, CA). One-way ANOVA and Tukey's HSD were used to determine statistical significance among treatments and p-values ≤ 0.05 were considered significant.

Results

Chemistry-dependent gp41-54Q-GHC kinetics and stabilization upon release from polyanhydride nanoparticles

The sizes of the 20:80 CPH:SA, 20:80 CPTEG:CPH and 50:50 CPTEG:CPH nanoparticles were 445 ± 230 nm, 179 ± 48 nm, and 231 ± 77 nm, respectively. The release profiles of gp41-54Q-GHC from these particles are shown in Figure 1. These data show that over 80% of the amount of gp41-54Q-GHC encapsulated within the particles was released within 30 days for all three formulations studied. Based upon the release profiles in Figure 1, there was a more pronounced "burst" release of the immunogen from the 20:80 CPH:SA nanoparticles within the first 72 h in comparison to the release from the CPTEG:CPH formulations. The amphiphilic 50:50 CPTEG:CPH formulation provided sustained release of the immunogen with a small burst. The encapsulation efficiency of gp41-54Q-GHC into the nanoparticles was chemistry-dependent with 79%, 70%, and 92% for 20:80 CPH:SA, 20:80 CPTEG:CPH, and 50:50 CPTEG:CPH, respectively. Analysis of released gp41-54Q-GHC via gel electrophoresis showed that bands consistent with the molecular weight of the non-encapsulated antigen (~14 kDa) were present in the polyacrylamide gels. As shown in Figure 1 the ~14 kDa protein band was present for the antigen released from all the nanoparticle formulations. However, the band corresponding to protein released from 50:50 CPTEG:CPH nanoparticles was more intense than that corresponding to protein released from 20:80 CPTEG:CPH or 20:80 CPH:SA nanoparticles. A small amount of degraded protein was visible in the lane corresponding to the 20:80 CPTEG:CPH nanoparticles. No low molecular weight bands were observed in the lanes corresponding to the other two chemistries. Based upon these results and upon our previous work, which suggested that amphiphilic formulations were more suitable for release of stable proteins [31, 41, 42, 50, 52], the 50:50 CPTEG:CPH nanoparticle formulation was chosen to perform the carbohydrate functionalization and DC activation studies.

Functionalization and characterization of carbohydrate-modified nanoparticles

The functionalization of gp41-54Q-GHC-loaded 50:50 CPTEG:CPH nanoparticles was carried out using the two-step amine-carboxylic acid coupling reaction. This reaction was carried out under aqueous conditions, which leads to partial degradation of the biodegradable nanoparticles, and loss of payload in the process. In order to minimize this loss, the total reaction time was varied from two to 18 hours and the resultant functionalized nanoparticles were characterized using QELS to measure zeta potential and the phenol sulfuric acid assay to quantify the amount of sugar attached to the surface of the

nanoparticles. The ζ-potential and the surface concentration of the sugars for each formulation are shown in Table 1. The NF particles are negatively charged, consistent with the presence of carboxylic acid moieties with a ζ-potential of −20 ± 2.6 mV, while the addition of the linker resulted in a positively charged surface with a ζ-potential of 23 ± 3.7 mV. The reaction time did not significantly affect the ζ-potential of the di-mannose-functionalized nanoparticles, suggesting that one hour for each coupling reaction was sufficient. Based upon these results, and because of the importance of minimizing the time that the nanoparticles were subject to aqueous conditions, a total reaction time of two hours for carbohydrate functionalization was used in subsequent studies.

gp41-54Q-GHC release kinetics from functionalized nanoparticles

Figure 2 shows the sustained release of gp41-54Q-GHC immunogen from NF, linker-, and di-mannose functionalized 50:50 CPTEG:CPH nanoparticles for 30 days. The data in Figure 2 shows that surface functionalization did not affect the cumulative release kinetics from the functionalized nanoparticles in comparison with the NF nanoparticles. The protein loss because of the exposure to aqueous conditions was observed to be 24–30% for the functionalized nanoparticles. All the formulations showed a small burst and >80% of the total amount of protein encapsulated in the nanoparticles was released from all the formulations.

gp41-54Q-GHC antigenicity was preserved upon release from functionalized nanoparticles

The antigenicity of the released gp41-54Q-GHC from the NF and functionalized 50:50 CPTEG:CPH nanoparticles was evaluated with an ELISA by using three broadly neutralizing monoclonal HIV-1 antibodies (2F5, Z13e1 and 4E10) and the results are shown in Figure 3. Samples of released protein after 1 h in PBS (pH 7.4) at 37°C were compared to non-encapsulated gp41-54Q-GHC. The relative antigenicity is defined as the ratio between the antigenicity of the released immunogen compared to that of the non-encapsulated immunogen. The data in Figure 3 demonstrate that the antigenicity of the immunogen released from all the formulations was preserved based on its recognition by all three monoclonal antibodies.

Internalization by DCs was enhanced by functionalization

The internalization of gp41-54Q-GHC-loaded polyanhydride nanoparticles by DCs was investigated using QDs to identify cells that were positive for nanoparticles. The internalization data in Figure 4 is expressed as the percentage of cells that were positive for the QDs. These results indicate that the internalization of the nanoparticles was enhanced by functionalization. In particular, DCs internalized both linker- and di-mannose-functionalized nanoparticles more than two-fold in comparison with the NF nanoparticles. About 3% of DCs internalized the NF 50:50 CPTEG:CPH nanoparticles, while ~6% of DCs internalized the linker- and di-mannose-functionalized nanoparticles. These results are consistent with previous studies in which CPTEG:CPH particles were internalized by bone marrow-derived DCs [54].

Functionalized nanoparticles enhanced DC expression of CD40 and CD206

DC activation was evaluated by stimulating bone marrow-derived DCs with gp41-54Q-GHC-containing nanoparticle formulations. Non-stimulated cells were used as a negative control and cells stimulated with LPS were used as a positive control. The up-regulation of MHC II, the co-stimulatory surface markers CD40 and CD86, and the CLR, CD206, was analyzed using flow cytometry. The data in Figure 5 is presented as the mean fluorescence intensity (MFI) from positive cells compared to isotypes for the marker of interest for each of the treatment groups. All the markers studied showed significant up-regulation compared to the negative control, as anticipated. Moreover, the data showed up-regulation of the co-stimulatory molecule CD40 and the CLR CD206 for cells stimulated with linker- and di-mannose-functionalized nanoparticles in comparison with NF nanoparticles as shown in Figure 5. The results also indicated that functionalization did not enhance the up-regulation of MHC II and the co-stimulatory molecule CD86 compared to the NF nanoparticles.

Functionalized nanoparticles modulated DC secretion of pro-inflammatory cytokines

The gp41-54Q-GHC-loaded nanoparticles were used to stimulate DCs and the supernatants were analyzed using a Bioplex assay to measure concentrations of the following cytokines: IL-6, IL-1β, TNF-α, IL-12p40, and IFN-γ. Figure 6 shows that cells stimulated with the functionalized nanoparticles secreted less IL-6 and TNF-α, compared to that of the NF treatment, specifically when gp41-54Q-GHC is loaded into the nanoparticles. There were no significant differences for IL-1β, IL-12p40, and IFN-γ secretion between cells stimulated with antigen-loaded NF and functionalized particles (data not shown). The cytokine secretion from DCs stimulated with all the nanoparticle treatments was enhanced significantly compared to the negative control.

Discussion

Surface functionalization of polymeric nanoparticles to achieve targeted delivery of antigen has been used to enhance vaccine efficacy by directing antigens to specific cells of the immune system [2,3,8,41–42,47,53]. Previous studies have shown that particle size, charge, shape, chemistry and surface functionality affect the immune response [28,31–32,40,47]. Therefore, rational design of particle-based adjuvants must involve optimization of these attributes to enhance the efficacy of the immune response. This strategy has also been utilized to mimic pathogenic signals in order to generate potent and protective immune responses [39–42]. In the current studies, the HIV-1 immunogen gp41-54Q-GHC was encapsulated into different polyanhydride formulations functionalized with carbohydrates and the stability of the released gp41-54Q-GHC and the effect of the functionalization on DC activation were investigated.

The HIV-1 antigen gp41-54Q-GHC was first encapsulated in three different polyanhydride nanoparticle formulations, i.e., 50:50 CPTEG:CPH, 20:80 CPTEG:CPH and 20:80 CPH:SA. These nanoparticles enabled sustained antigen release kinetics and provided an appropriate environment to preserve the primary structure of gp41-54Q-GHC. Released protein from 50:50 CPTEG:CPH nanoparticles displayed a more intense band after gel electrophoretic analysis when compared to the other formulations. This result combined with the high

encapsulation efficiency of the protein and the amphiphilic properties of this copolymer suggested that this chemistry was the most appropriate to stabilize gp41-54Q-GHC [30,31,53]; accordingly, this chemistry was chosen for further studies with carbohydrate functionalization and DC activation.

The functionalization of antigen-loaded polyanhydride nanoparticles was optimized and the total reaction time was reduced to two hours with 24–30% loss of immunogen during the process. As shown in Figure 2, the release kinetics of gp41-54Q-GHC from the different polyanhydride nanoparticle formulations displayed similar behavior, independent of the type of functionalization (i.e., linker and di-mannose) and was consistent with the release of the immunogen from the NF nanoparticles [29]. All these formulations provided sustained release of gp41-54Q-GHC, which is a desirable attribute for vaccine formulations. This is because it has been demonstrated previously that prolonging the presence of antigen in the host can improve the generation of antigen-specific memory cells that can trigger potent immune responses towards future infections [19,32].

The gp41-54Q-GHC immunogen released from the functionalized polyanhydride nanoparticles maintained its antigenic activity upon release, which was tested by its ability to bind to three monoclonal HIV-1 antibodies: 2F5, 4E10 and Z13e1 (Figure 3). The slight increase in the relative antigenicity of the protein released from the NF nanoparticles with the 2F5 antibody and that released from all the nanoparticle formulations with the 4E10 antibody may be attributed to minor conformational changes of the antigen after encapsulation and release, as observed previously [31,52–53,62–63]. These results indicated that the functionalization process did not significantly affect the antigenicity of gp41-54Q-GHC upon release. The small changes in antigenicity, if any, may be attributable to the encapsulation and release processes, as shown previously [31,52–53,63–64].

It is known that cells internalize positively charged nanoparticles more effectively than neutral or negatively charged nanoparticles [2–3,8]. Previous studies have demonstrated the effect of surface charge on particle internalization and the results from the current studies are consistent with these studies [39–41]. Functionalization with linker results in positively charged nanoparticles, which were internalized more efficiently by DCs, as shown in Figure 4. There were significant differences in cells positive for nanoparticles between the functionalized and the NF nanoparticles, indicating the importance of surface charge and/or specific internalization pathways (i.e., mannose receptor-mediated endocytosis) with respect to particle uptake. The enhanced internalization was observed for both the di-mannose- and the linker-functionalized nanoparticles, suggesting that surface charge may be more important than receptor-mediated uptake. On the other hand, previous work has shown that targeting specific receptors such as the macrophage mannose receptor by functionalizing nanoparticles with carbohydrates such as di-mannose resulted in enhanced APC activation [39–41,48]. Based on these observations and the current work, it is hypothesized that combinatorial use of both surface charge and functionalization with ligands that target specific CLRs may be important for enhanced internalization of the functionalized nanoparticles. This enhanced internalization can lead to the efficient delivery of antigen to the APCs, which is important for the induction of robust T cell-mediated immune responses [2–3,40,65]. It is important to note even though only a small percentage of cells were

positive for CPTEG-containing particles *in vitro*, antigen-encapsulated 50:50 CPTEG:CPH formulations have been shown in previous studies to induce protective immunity to a subsequent live challenge [32,34]. In addition, it has been hypothesized that HIV-1 infection of DCs via dendritic cell-specific intercellular adhesion molecule-3-grabbing non-integrin (DC-SIGN) may cause DC-DC viral transmission, or DC-T cell infection amplification [66,67]. In addition, it is known that DC-SIGN$^+$ immature DCs, which are located in vaginal, cervical and rectal mucosa, are the first type of cells to encounter the HIV-1 virion [68]. It is also known that DC-SIGN captures HIV-1 in the periphery and facilitates its transport to secondary lymphoid organs rich in T cells [66]. While these functions are performed by DC-SIGN in DCs, they are performed by the MMR in macrophages and epithelial DCs, which are present at mucosal surfaces [68, 69]. In this regard, surface functionalization of nanoparticle-based vaccines or anti-viral delivery vehicles with carbohydrates offers the possibility to target CLRs such as the MMR or DC-SIGN in macrophages or dendritic cells.

The appropriate activation of APCs is an important component of an immune response towards pathogens [1,16,47–48,50]. Specifically, during HIV-1 infection, DCs and macrophages play critical roles in the induction of robust and balanced immune responses [1–2,14–16,19,22–23]. Even though DC-SIGN has been identified as a key player in HIV-1 infection, the presence of the MMR on epithelial DCs and macrophages offers the possibility to specifically target nanovaccines and/or anti-viral delivery vehicles towards these cellular populations, since mucosal vaccination has been shown to elicit antibodies across these surfaces, specifically in vaginal and genital tissues [70]. Therefore, up-regulation of APC activation markers, including CD206, is a desirable characteristic of adjuvants used in conjunction with an HIV-1 vaccine [25,52–53]. All the nanoparticle formulations studied herein enhanced the DC surface expression of MHC II, the co-stimulatory molecules CD40 and CD86, and the CLR CD206 compared to non-stimulated cells (Figure 5). While cells stimulated with the carbohydrate-functionalized nanoparticles showed enhanced expression of CD40 and CD206 compared to cells stimulated with NF nanoparticles, the surface expression of CD86 and MHC II were similar in cells stimulated by both NF and functionalized nanoparticles. The MFI of cells stimulated with the gp41-54Q-GH-encapsulated nanoparticles was higher than that of the cells stimulated by the NF nanoparticles, regardless of functionalization (data not shown). The enhanced expression of CD40 and CD206 is consistent with the internalization data of Figure 4 because it has been shown previously that particle uptake is required for the up-regulation of these molecules [41–42]. It is known that CD40 is important for DC maturation that drives T cell activation, while CD206-mediated antigen delivery has been shown to enhance humoral immune responses [1,2,10,65,71]. These characteristics are desirable when designing an HIV-1 vaccine due to the important role of a balanced immune response involving both cellular and humoral components [19,72]. The results in Figure 5 also indicated that functionalization did not enhance the up-regulation of MHC II and the co-stimulatory molecule CD86 compared to the NF nanoparticles. This observation suggests the presence of a bystander effect, which enables cells that are in close proximity with nanoparticles to enhance their surface expression of MHC II and CD86, rendering nanoparticle

internalization unnecessary [48,54]. These data are consistent with previous studies that also postulated a bystander effect for up-regulation of MHC II and CD86 [48,54].

Nanoparticle functionalization modulated cytokine secretion by DCs, as shown in Figure 6. The secretion of IL-1β, IL-12p40 and IFN-γ was similar in cells stimulated by NF or functionalized nanoparticles. In contrast, the DC secretion of IL-6 and TNF-α was higher when stimulated with the NF nanoparticles in contrast to the functionalized nanoparticles. This observation may be attributed to the higher amount of antigen present in the NF nanoparticles compared to that in the functionalized nanoparticles. These results are consistent with the mass of gp41-54Q-GHC released from the nanoparticles within the first 72 h as shown in Figure 6. In control experiments, it was demonstrated that the antigen-containing nanoparticles (regardless of functionalization or lack thereof) resulted in higher cytokine secretion than their respective “blank” (i.e., no antigen) counterparts. The antigen-dependent response of cytokine secretion suggests that the higher amount of protein encapsulated within the NF nanoparticles compared to the carbohydrate-functionalized nanoparticles may be important and is consistent with previous observations [5]. The presence of antigen within the particles appears to be more important for IL-6 and TNF-α secretion than for the secretion of IL-1β, IL-12p40 and IFN-γ. These results are consistent with previous work, in which it has been shown that when targeting specific CLRs such as SIGNR1, there is a decrease in the secretion of cytokines such as IL-6 or TNF-α [73,74]. It has also been shown using a colitis model that deficiency of this receptor results in a decrease in the secretion of these cytokines [75]. These results suggest that creating combinations of NF and functionalized nanoparticle formulations may provide the benefits of enhanced internalization, up-regulation of cell surface markers, and enhanced secretion of the appropriate cytokines, all of which will lead to potent immune responses.

The current experiments demonstrate that polyanhydride nanoparticles can serve as a promising adjuvant and/or delivery system for an HIV-1 nanovaccine. The studies provide important insights upon the behavior of APCs when stimulated with nanoparticles of different chemistries, surface charge, functionalization, and antigen encapsulation. Such insights are valuable for the rational design of adjuvants/delivery vehicles for vaccine development. The desirable characteristics of the polyanhydride nanoparticle platform include the provision of antigen stability, sustained release, enhanced particle uptake, and DC activation. Carbohydrate functionalization of the nanoparticles enhanced their adjuvant capabilities by enabling charge and receptor-mediated uptake mechanisms. The current studies demonstrate the potential of using functionalized polyanhydride nanoparticles as an adjuvant/delivery vehicle for HIV-1 antigens and provide the opportunity to tailor specific properties to lead to efficacious immune responses downstream.

Conclusions

In these studies, carbohydrate-functionalized polyanhydride nanoparticles were investigated as targeted antigen delivery vehicles and adjuvants for gp41-54Q-GHC, an HIV-1 antigen. Polymer chemistry, surface functionalization, and antigen encapsulation were analyzed and their effect on DC activation was evaluated. The results demonstrated that amphiphilic polyanhydride nanoparticles released antigenic gp41-54Q-GHC and that functionalization

enhanced particle internalization. Functionalization also enhanced the up-regulation of DC activation markers, while regulating cytokine secretion. These data offer important insights into the performance of functionalized nanoparticles with respect to releasing stable HIV-1 immunogens and activating DCs. Active targeting of these nanoparticles by functionalization with carbohydrates offers a promising opportunity to design efficacious vaccine delivery systems for HIV-1.

Acknowledgments

The authors acknowledge financial support from NIH-NIAID (U19 AI-091031). The authors acknowledge useful discussions with Dr. Michael J. Wannemuehler on the DC activation data and thank Shawn Rigby of the Iowa State University Flow Cytometry facility for his assistance with the flow cytometry experiments. MWC has an equity interest in NeoVaxSyn Incorporated, and serves as CEO/President. NeoVaxSyn Inc. did not contribute to this work or to the interpretation of the data. The following reagents were obtained through the NIH AIDS Reagent Program, Division of AIDS, NIAID, NIH: HIV-1 gp41 mAb 2F5, 4E10 and Z13e1.

References

1. Geijtenbeek TB, Gringhuis SI. Signalling through C-type lectin receptors: shaping immune responses. Nat Rev Immunol. 2009; 9:465–479. [PubMed: 19521399]
2. Keler T, Ramakrishna V, Fanger MW. Mannose receptor-targeted vaccines. Expert Opin Biol Ther. 2004; 4:1953–1962. [PubMed: 15571457]
3. Irache JM, Salman HH, Gamazo C, Espuelas S. Mannose-targeted systems for the delivery of therapeutics. Expert Opin Drug Deliv. 2008; 5:703–724. [PubMed: 18532925]
4. Deng Z, Li S, Jiang X, Narain R. Well-defined galactose-containing multi-functional copolymers and glyconanoparticles for biomolecular recognition processes. Macromolecules. 2009; 42:6393–6405.
5. Song EH, Osanya AO, Petersen CA, Pohl NL. Synthesis of multivalent tuberculosis and Leishmania-associated capping carbohydrates reveals structure-dependent responses allowing immune evasion. J Am Chem Soc. 2010; 132:11428–11430. [PubMed: 20669964]
6. Engering AJ, Cella M, Fluitsma D, Brockhaus M, Hoefsmit EC, Lanzavecchia A, et al. The mannose receptor functions as a high capacity and broad specificity antigen receptor in human dendritic cells. Eur J Immunol. 1997; 27:2417–2425. [PubMed: 9341788]
7. Upham JP, Pickett D, Irimura T, Anders EM, Reading PC. Macrophage receptors for influenza A virus: role of the macrophage galactose-type lectin and mannose receptor in viral entry. J Virol. 2010; 84:3730–3737. [PubMed: 20106926]
8. Jiang HL, Kang ML, Quan JS, Kang SG, Akaike T, Yoo HS, et al. The potential of mannosylated chitosan microspheres to target macrophage mannose receptors in an adjuvant-delivery system for intranasal immunization. Biomaterials. 2008; 29:1931–1939. [PubMed: 18221992]
9. Figdor CG, van Kooyk Y, Adema GJ. C-type lectin receptors on dendritic cells and Langerhans cells. Nat Rev Immunol. 2002; 2:77–84. [PubMed: 11910898]
10. Cambi A, Figdor CG. Dual function of C-type lectin-like receptors in the immune system. Curr Opin Cell Biol. 2003; 15:539–546. [PubMed: 14519388]
11. Stahl PD. The mannose receptor and other macrophage lectins. Curr Opin Immunol. 1992; 4:49–52. [PubMed: 1317711]
12. Pyz E, Marshall AS, Gordon S, Brown GD. C-type lectin-like receptors on myeloid cells. Ann Med. 2006; 38:242–251. [PubMed: 16754255]
13. Chehimi J, Luo Q, Azzoni L, Shawver L, Ngoubilly N, June R, et al. HIV-1 transmission and cytokine-induced expression of DC-SIGN in human monocyte-derived macrophages. J Leukoc Biol. 2003; 74:757–7sss63. [PubMed: 12960240]
14. Herbein G, Gras G, Khan KA, Abbas W. Macrophage signaling in HIV-1 infection. Retrovirology. 2010; 7:34. [PubMed: 20380698]

15. Gringhuis SI, van der Vlist M, van den Berg LM, den Dunnen J, Litjens M, Geijtenbeek TB. HIV-1 exploits innate signaling by TLR8 and DC-SIGN for productive infection of dendritic cells. Nat Immunol. 2010; 11:419–426. [PubMed: 20364151]
16. Mascola JR, Montefiori DC. The role of antibodies in HIV vaccines. Annu Rev Immunol. 2010; 28:413–444. [PubMed: 20192810]
17. Zolla-Pazner S. Identifying epitopes of HIV-1 that induce protective antibodies. Nat Rev Immunol. 2004; 4:199–210. [PubMed: 15039757]
18. UNAIDS. Global report: UNAIDS report on the global AIDS epidemic 2010. 2010
19. McMichael AJ, Borrow P, Tomaras GD, Goonetilleke N, Haynes BF. The immune response during acute HIV-1 infection: clues for vaccine development. Nat Rev Immunol. 2010; 10:11–23. [PubMed: 20010788]
20. Catalfamo M, Di Mascio M, Hu Z, Srinivasula S, Thaker V, Adelsberger J, et al. HIV infection-associated immune activation occurs by two distinct pathways that differentially affect CD4 and CD8 T cells. Proc Natl Acad Sci U S A. 2008; 105:19851–19856. [PubMed: 19060209]
21. Karlsson Hedestam GB, Fouchier RA, Phogat S, Burton DR, Sodroski J, Wyatt RT. The challenges of eliciting neutralizing antibodies to HIV-1 and to influenza virus. Nat Rev Microbiol. 2008; 6:143–155. [PubMed: 18197170]
22. Nguyen DG, Hildreth JE. Involvement of macrophage mannose receptor in the binding and transmission of HIV by macrophages. Eur J Immunol. 2003; 33:483–493. [PubMed: 12645947]
23. Sol-Foulon N, Moris A, Nobile C, Boccaccio C, Engering A, Abastado JP, et al. HIV-1 NEF-induced upregulation of DC-SIGN in dendritic cells promotes lymphocyte clustering and viral spread. Immunity. 2002; 16:145–155. [PubMed: 11825573]
24. Geijtenbeek TB, Kwon DS, Torensma R, van Vliet SJ, van Duijnhoven GC, Middel J, et al. DC-SIGN, a dendritic cell-specific HIV-1-binding protein that enhances trans-infection of T cells. Cell. 2000; 100:587–597. [PubMed: 10721995]
25. Scanlan CN, Offer J, Zitzmann N, Dwek RA. Exploiting the defensive sugars of HIV-1 for drug and vaccine design. Nature. 2007; 446:1038–1045. [PubMed: 17460665]
26. Shi W, Bohon J, Han DP, Habte H, Qin Y, Cho MW, et al. Structural characterization of HIV gp41 with the membrane-proximal external region. J Biol Chem. 2010; 285:24290–24298. [PubMed: 20525690]
27. Conix A. Poly[1,3-bis(*p*-carboxyphenoxy)-propane anhydride]. Macromolecular Synthesis. 1966; 2:95–98.
28. Kumar N, Langer RS, Domb AJ. Polyanhydrides: an overview. Adv Drug Deliv Rev. 2002; 54:889–910. [PubMed: 12384314]
29. Torres MP, Vogel BM, Narasimhan B, Mallapragada SK. Synthesis and characterization of novel polyanhydrides with tailored erosion mechanisms. J Biomed Mater Res A. 2006; 76:102–110. [PubMed: 16138330]
30. Petersen LK, Sackett CK, Narasimhan B. High-throughput analysis of protein stability in polyanhydride nanoparticles. Acta Biomater. 2010; 6:3873–3881. [PubMed: 20388561]
31. Carrillo-Conde B, Schiltz E, Yu J, Chris Minion F, Phillips GJ, Wannemuehler MJ, et al. Encapsulation into amphiphilic polyanhydride microparticles stabilizes Yersinia pestis antigens. Acta Biomater. 2010; 6:3110–3119. [PubMed: 20123135]
32. Ulery BD, Kumar D, Ramer-Tait AE, Metzger DW, Wannemuehler MJ, Narasimhan B. Design of a protective single-dose intranasal nanoparticle-based vaccine platform for respiratory infectious diseases. PLoS One. 2011; 6:17642.
33. Kipper MJ, Wilson JH, Wannemuehler MJ, Narasimhan B. Single dose vaccine based on biodegradable polyanhydride microspheres can modulate immune response mechanism. J Biomed Mater Res A. 2006; 76:798–810. [PubMed: 16345084]
34. Ulery BD, Petersen LK, Phanse Y, Kong CS, Broderick SR, Kumar D, et al. Rational design of pathogen-mimicking amphiphilic materials as nanoadjuvants. Sci Rep. 2011; 1:198. [PubMed: 22355713]
35. Penn-Nicholson A, Han DP, Kim SJ, Park H, Ansari R, Montefiori DC, et al. Assessment of antibody responses against gp41 in HIV-1-infected patients using soluble gp41 fusion proteins and

peptides derived from M group consensus envelope. Virology. 2008; 372:442–456. [PubMed: 18068750]

36. Gaiha GD, Dong T, Palaniyar N, Mitchell DA, Reid KB, Clark HW. Surfactant protein A binds to HIV and inhibits direct infection of CD4+ cells, but enhances dendritic cell-mediated viral transfer. J Immunol. 2008; 181:601–609. [PubMed: 18566427]
37. Fantuzzi L, Canini I, Belardelli F, Gessani S. HIV-1 gp120 stimulates the production of beta-chemokines in human peripheral blood monocytes through a CD4-independent mechanism. J Immunol. 2001; 166:5381–5387. [PubMed: 11313374]
38. Shan M, Klasse PJ, Banerjee K, Dey AK, Iyer SP, Dionisio R, et al. HIV-1 gp120 mannoses induce immunosuppressive responses from dendritic cells. PLoS Pathog. 2007; 3:169.
39. Shen E, Pizsczek R, Dziadul B, Narasimhan B. Microphase separation in bioerodible copolymers for drug delivery. Biomaterials. 2001; 22:201–210. [PubMed: 11197495]
40. Torres MP, Wilson-Welder JH, Lopac SK, Phanse Y, Carrillo-Conde B, Ramer-Tait AE, et al. Polyanhydride microparticles enhance dendritic cell antigen presentation and activation. Acta Biomater. 2011; 7:2857–2864. [PubMed: 21439412]
41. Kipper MJ, Shen E, Determan A, Narasimhan B. Design of an injectable system based on bioerodible polyanhydride microspheres for sustained drug delivery. Biomaterials. 2002; 23:4405–4412. [PubMed: 12219831]
42. Ulery BD, Phanse Y, Sinha A, Wannemuehler MJ, Narasimhan B, Bellaire BH. Polymer chemistry influences monocytic uptake of polyanhydride nanospheres. Pharm Res. 2009; 26:683–690. [PubMed: 18987960]
43. Jaipuri FA, Pohl NL. Toward solution-phase automated iterative synthesis: fluorous-tag assisted solution-phase synthesis of linear and branched mannose oligomers. Org Biomol Chem. 2008; 6:2686–2691. [PubMed: 18633525]
44. Curran DP, Luo Z. Fluorous synthesis with fewer fluorines (light fluorous synthesis): Separation of tagged from untagged products by solid-phase extraction with fluorous reverse-phase silica gel. J Amer Chem Soc. 1999; 121:9069–9072.
45. Zhang W. Fluorous linker-facilitated chemical synthesis. Chem Rev. 2009; 109:749–795. [PubMed: 19146385]
46. Zhang W, Curran DP. Synthetic applications of fluorous solid-phase extraction (F-SPE). Tetrahedron. 2006; 62:11837–11865. [PubMed: 18509513]
47. Carrillo-Conde B, Song EH, Chavez-Santoscoy A, Phanse Y, Ramer-Tait AE, Pohl NL, et al. Mannose-functionalized “pathogen-like” polyanhydride nanoparticles target C-type lectin receptors on dendritic cells. Mol Pharm. 2011; 8:1877–1886. [PubMed: 21882825]
48. Chavez-Santoscoy AV, Roychoudhury R, Pohl NL, Wannemuehler MJ, Narasimhan B, Ramer-Tait AE. Tailoring the immune response by targeting C-type lectin receptors on alveolar macrophages using “pathogen-like” amphiphilic polyanhydride nanoparticles. Biomaterials. 2012; 33:4762–4772. [PubMed: 22465338]
49. Carrillo-Conde BR, Roychoudhury R, Chavez-Santoscoy AV, Narasimhan B, Pohl NL. High-throughput synthesis of carbohydrates and functionalization of polyanhydride nanoparticles. J Vis Exp. 2012; 64:3884. [PubMed: 22710268]
50. Phanse Y, Carrillo-Conde BR, Ramer-Tait AE, Roychoudhury R, Pohl NL, Narasimhan B, et al. Functionalization of polyanhydride microparticles with di-mannose influences uptake by and intracellular fate within dendritic cells. Acta Biomater. 2013; 9:8902–8909. [PubMed: 23796408]
51. Masuko T, Minami A, Iwasaki N, Majima T, Nishimura S, Lee YC. Carbohydrate analysis by a phenol-sulfuric acid method in microplate format. Anal Biochem. 2005; 339:69–72. [PubMed: 15766712]
52. Lopac SK, Torres MP, Wilson-Welder JH, Wannemuehler MJ, Narasimhan B. Effect of polymer chemistry and fabrication method on protein release and stability from polyanhydride microspheres. J Biomed Mater Res B Appl Biomater. 2009; 91:938–947. [PubMed: 19642209]
53. Torres MP, Determan AS, Anderson GL, Mallapragada SK, Narasimhan B. Amphiphilic polyanhydrides for protein stabilization and release. Biomaterials. 2007; 28:108–116. [PubMed: 16965812]

54. Carrillo-Conde BR, Ramer-Tait AE, Wannemuehler MJ, Narasimhan B. Chemistry-dependent adsorption of serum proteins onto polyanhydride microparticles differentially influences dendritic cell uptake and activation. Acta Biomater. 2012; 8:3618–3628. [PubMed: 22684115]
55. Buchacher A, Predl R, Strutzenberger K, Steinfellner W, Trkola A, Purtscher M, et al. Generation of human monoclonal antibodies against HIV-1 proteins; electrofusion and Epstein-Barr virus transformation for peripheral blood lymphocyte immortalization. AIDS Res Hum Retroviruses. 1994; 10:359–369. [PubMed: 7520721]
56. Purtscher M, Trkola A, Grassauer A, Schulz PM, Klima A, Döpper S, et al. Restricted antigenic variability of the epitope recognized by the neutralizing gp41 antibody 2F5. AIDS. 1996; 10:587–593. [PubMed: 8780812]
57. Purtscher M, Trkola A, Gruber G, Buchacher A, Predl R, Steindl F, et al. A broadly neutralizing human monoclonal antibody against gp41 of human immunodeficiency virus type 1. AIDS Res Hum Retroviruses. 1994; 10:1651–1658. [PubMed: 7888224]
58. Nelson JD, Brunel FM, Jensen R, Crooks ET, Cardoso RM, Wang M, et al. An affinity-enhanced neutralizing antibody against the membrane-proximal external region of human immunodeficiency virus type 1 gp41 recognizes an epitope between those of 2F5 and 4E10. J Virol. 2007; 81:4033–4043. [PubMed: 17287272]
59. Stiegler G, Kunert R, Purtscher M, Wolbank S, Voglauer R, Steindl F, et al. A potent cross-clade neutralizing human monoclonal antibody against a novel epitope on gp41 of human immunodeficiency virus type 1. AIDS Res Hum Retroviruses. 2001; 17:1757–1765. [PubMed: 11788027]
60. Zwick MB, Labrijn AF, Wang M, Spenlehauer C, Saphire EO, Binley JM, et al. Broadly neutralizing antibodies targeted to the membrane-proximal external region of human immunodeficiency virus type 1 glycoprotein gp41. J Virol. 2001; 75:10892–10905. [PubMed: 11602729]
61. Petersen LK, Xue L, Wannemuehler MJ, Rajan K, Narasimhan B. The simultaneous effect of polymer chemistry and device geometry on the in vitro activation of murine dendritic cells. Biomaterials. 2009; 30:5131–5142. [PubMed: 19539989]
62. Petersen LK, Ramer-Tait AE, Broderick SR, Kong CS, Ulery BD, Rajan K, et al. Activation of innate immune responses in a pathogen-mimicking manner by amphiphilic polyanhydride nanoparticle adjuvants. Biomaterials. 2011; 32:6815–68ss22. [PubMed: 21703679]
63. Determan AS, Graham JR, Pfeiffer KA, Narasimhan B. The role of microsphere fabrication methods on the stability and release kinetics of ovalbumin encapsulated in polyanhydride microspheres. J Microencapsul. 2006; 23:832–843. [PubMed: 17390625]
64. Petersen LK, Phanse Y, Ramer-Tait AE, Wannemuehler MJ, Narasimhan B. Amphiphilic polyanhydride nanoparticles stabilize *Bacillus anthracis* protective antigen. Mol Pharm. 2012; 9:874–882. [PubMed: 22380593]
65. Adams EW, Ratner DM, Seeberger PH, Hacohen N. Carbohydrate-mediated targeting of antigen to dendritic cells leads to enhanced presentation of antigen to T cells. Chembiochem. 2008; 9:294–303. [PubMed: 18186095]
66. Turville S, Wilkinson J, Cameron P, Dable J, Cunningham AL. The role of dendritic cell C-type lectin receptors in HIV pathogenesis. J Leukoc Biol. 2003; 74:710–718. [PubMed: 12960229]
67. Berzi A, Varga N, Sattin S, Antonazzo P, Biasin M, Cetin I, et al. Pseudo-mannosylated DC-SIGN ligands as potential adjuvants for HIV vaccines. Viruses. 2014; 6:391–403. [PubMed: 24473338]
68. Jameson B, Baribaud F, Pohlmann S, Ghavimi D, Mortari F, Doms RW, et al. Expression of DC-SIGN by dendritic cells of intestinal and genital mucosae in humans and rhesusmacaques. J Virol. 2002; 76:1866–1875. [PubMed: 11799181]
69. Cunningham AL, Harman AN, Donaghy H. DC-SIGN ‘AIDS’ HIV immune evasion and infection. Nat Immunol. 2007; 8:556–558. [PubMed: 17514207]
70. Holmgren J, Czerkinsky C. Mucosal immunity and vaccines. Nature medicine. 2005; 11:45–53.
71. Elgueta R, Benson MJ, de Vries VC, Wasiuk A, Guo Y, Noelle RJ. Molecular mechanism and function of CD40/CD40L engagement in the immune system. Immunol Rev. 2009; 229:152–172. [PubMed: 19426221]

72. McKenzie EJ, Taylor PR, Stillion RJ, Lucas AD, Harris J, Gordon S, et al. Mannose receptor expression and function define a new population of murine dendritic cells. J Immunol. 2007; 178:4975–4983. [PubMed: 17404279]

73. Ohtani M, Iyori M, Saeki A, Tanizume N, Into T, Hasebe A, et al. Involvement of suppressor of cytokine signalling-1-mediated degradation of MyD88-adaptor-like protein in the suppression of Toll-like receptor 2-mediated signalling by the murine C-type lectin SIGNR1-mediated signalling. Cellular microbiology. 2012; 14:40–57. [PubMed: 21899704]

74. Lewis JS, Zaveri TD, Crooks CP 2nd, Keselowsky BG. Microparticle surface modifications targeting dendritic cells for non-activating applications. Biomaterials. 2012; 33:7221–7232. [PubMed: 22796161]

75. Saunders SP, Barlow JL, Walsh CM, Bellsoi A, Smith P, McKenzie AN, et al. C-type lectin SIGN-R1 has a role in experimental colitis and responsiveness to lipopolysaccharide. J.Immunol. 2010; 184:2627–2637. [PubMed: 20130211]

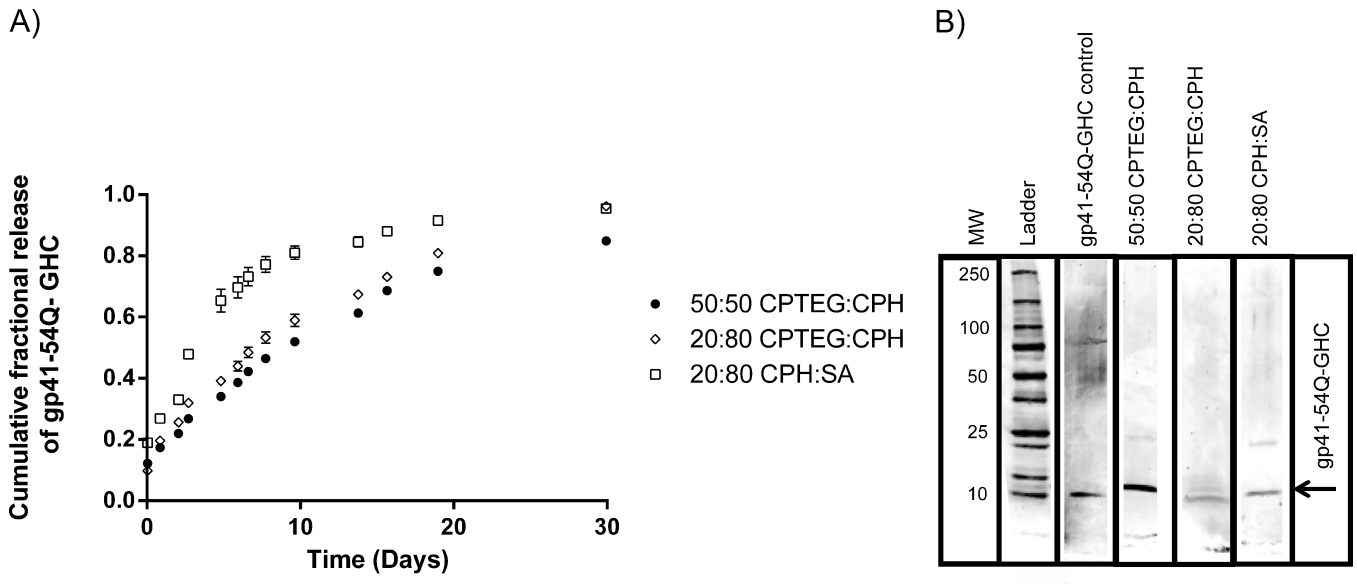

Figure 1.

gp41-54Q-GHC antigen release kinetics from polyanhydride nanoparticles and structural stability upon release. A) Cumulative fraction of gp41-54Q-GHC released from (●) 50:50 CPTEG:CPH, (×) 20:80 CPTEG:CPH and (▫) 20:80 CPH:SA nanoparticles. Error bars represent standard error of the mean; results are representative of two independent experiments with duplicate samples used in each experiment. B) Primary structure analysis of released gp41-54Q-GHC by gel electrophoresis. Samples were analyzed after one hour of release from 50:50 CPTEG:CPH, 20:80 CPTEG:CPH and 20:80 CPH:SA nanoparticles.

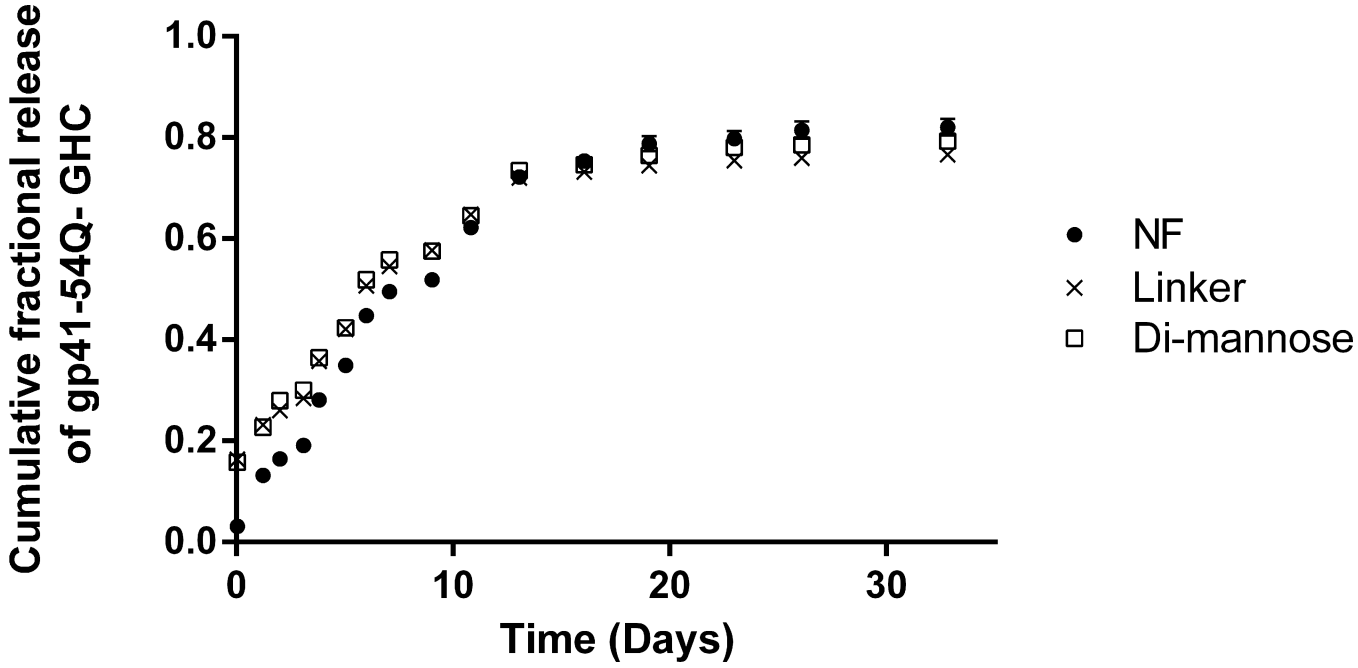

Figure 2.

Cumulative fraction of gp41-54Q-GHC released from (●) NF, (×) linker- and (□) di-mannose-functionalized 50:50 CPTEG:CPH nanoparticles. Error bars represent standard error of the mean; results are representative of two independent experiments with duplicate samples used in each experiment.

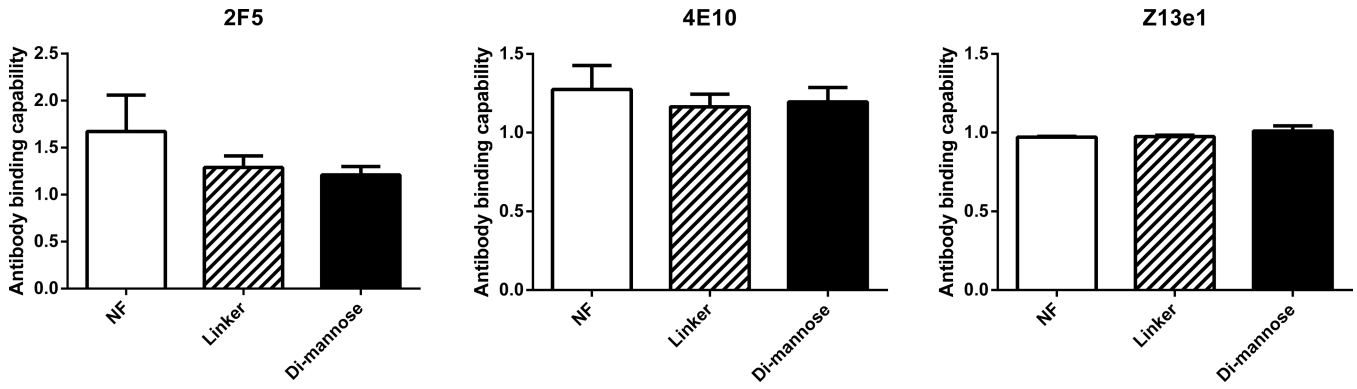

Figure 3.

Antigenic analysis of released gp41-54Q-GHC at 37°C from NF, linker-, and di-mannose-functionalized 50:50 CPTEG:CPH nanoparticles. Antibody binding capability was measured by ELISA using three HIV monoclonal antibodies: Z13e1, 2F5, and 4E10. Error bars represent standard error of the mean from results obtained from two independent experiments with triplicate samples in each experiment.

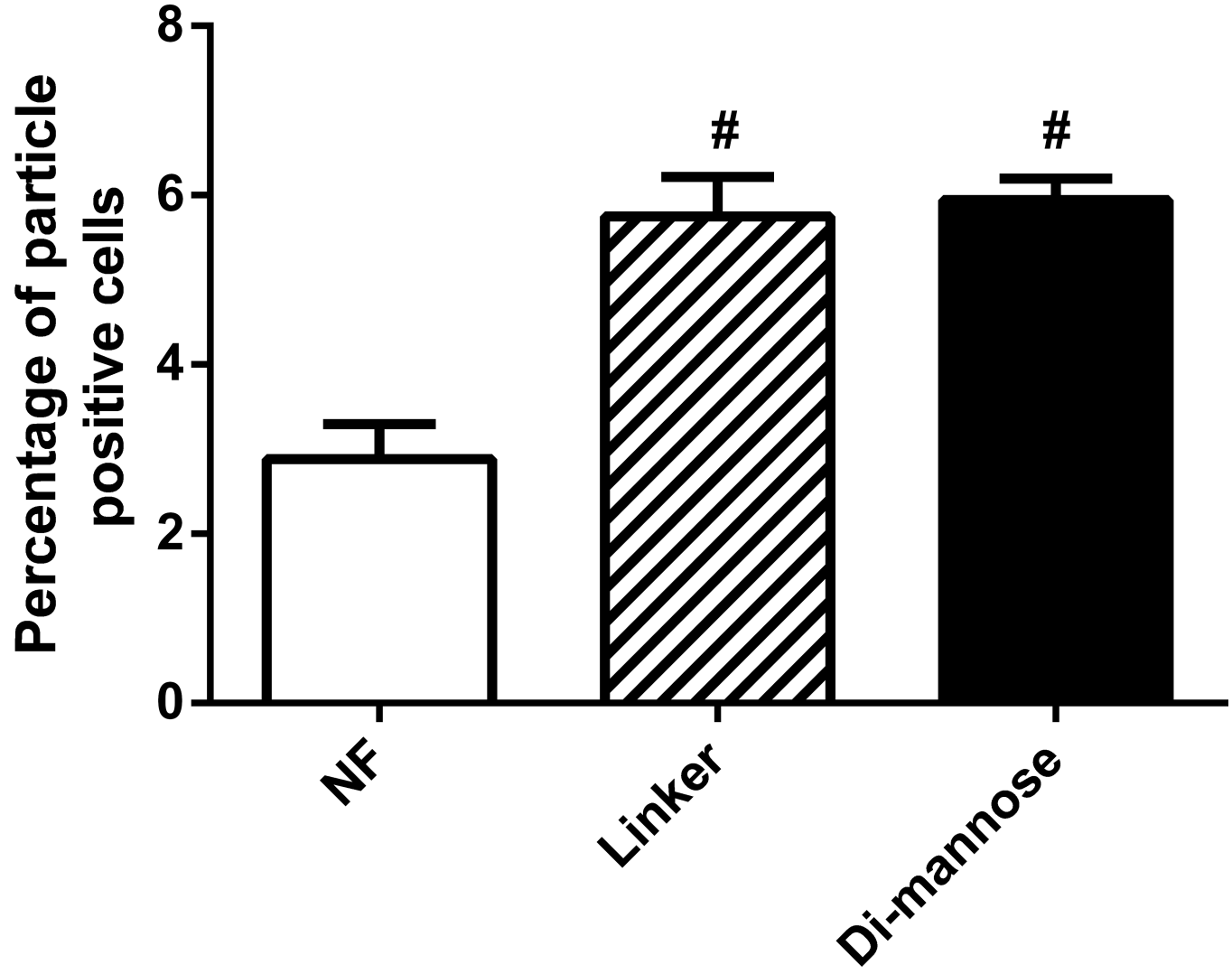

Figure 4.

Cellular internalization was enhanced by positively charged polyanhydride nanoparticles. The internalization by DCs of QD-loaded NF, linker-, and di-mannose-functionalized nanoparticles was analyzed using flow cytometry. Error bars represent standard error of the mean; results are representative of three independent experiments with triplicate samples used in each experiment.

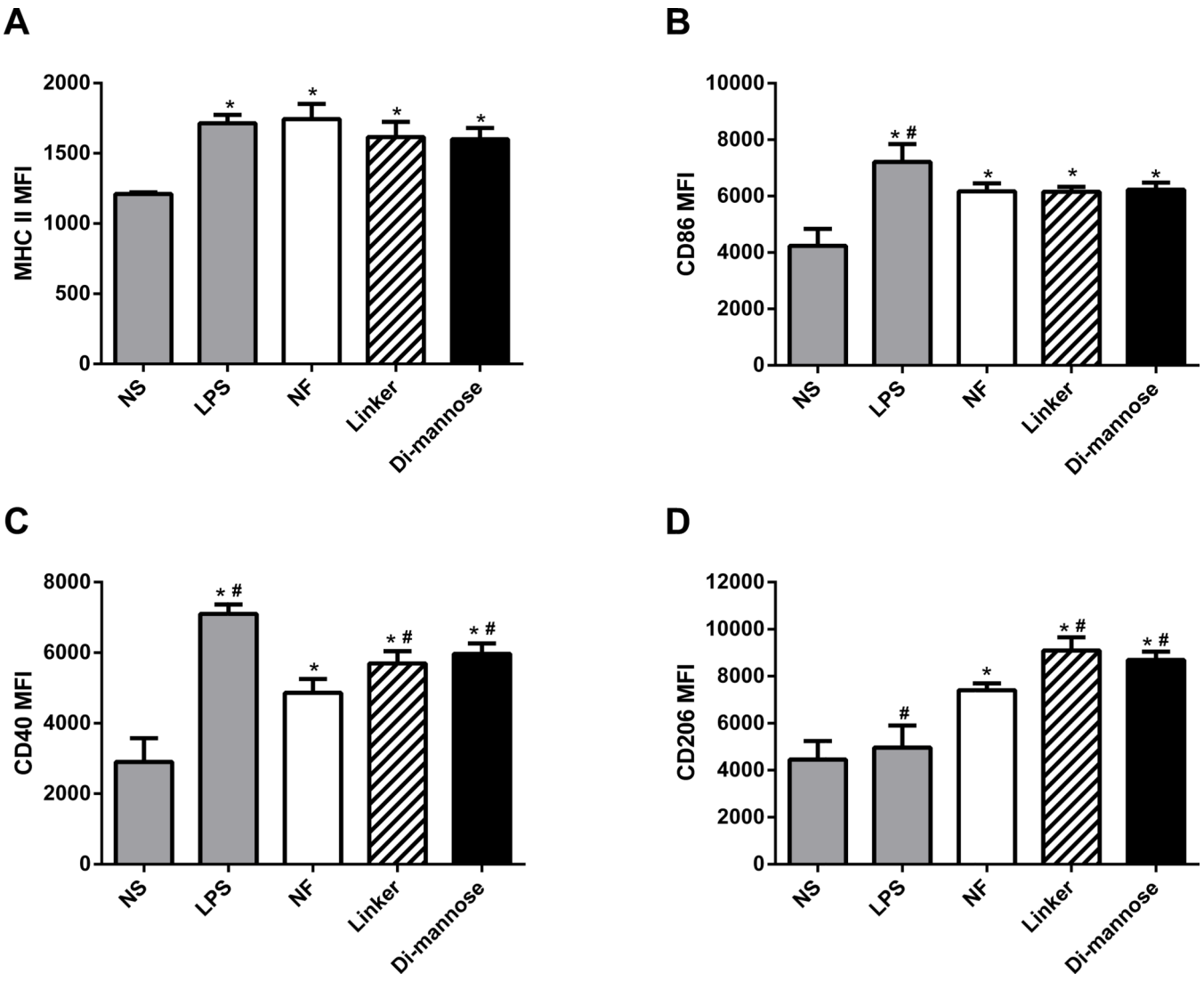

Figure 5.

Di-mannose-functionalized nanoparticles enhanced DC expression of co-stimulatory molecules and CLRs. After stimulation with either 125 μg/mL of NF or functionalized nanoparticles for 48 h, DCs were harvested and analyzed by flow cytometry for surface expression of MHC II, CD86, CD40, and CD206. LPS-stimulated and non-stimulated cells (NS) were used as positive and negative controls, respectively. Data are expressed as the mean ± SEM of three independent experiments performed in triplicate. * and # represent groups that are statistically significant ($p \leq 0.05$) compared to the NS or NF groups, respectively. MFI = mean fluorescence intensity.

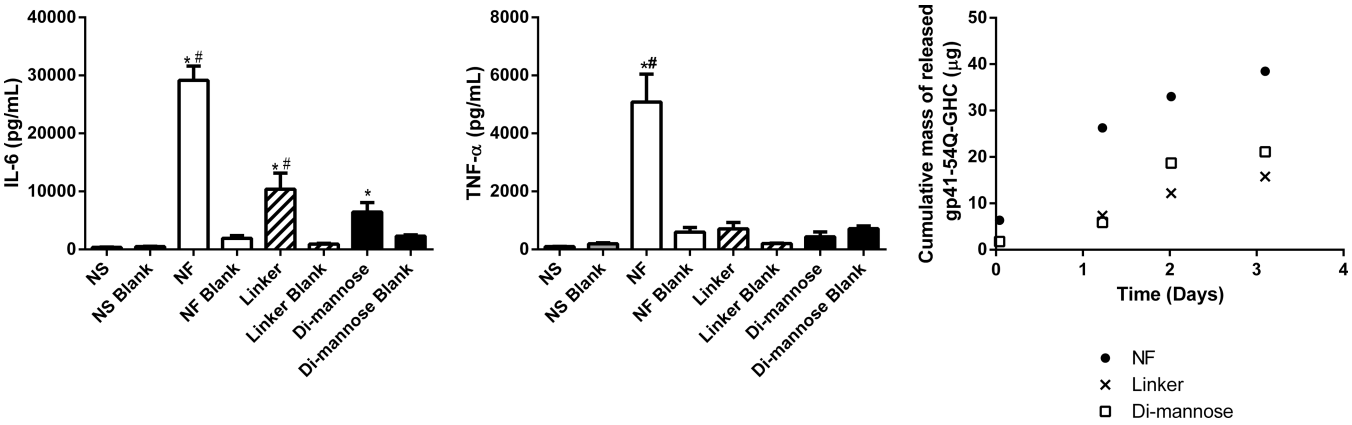

Figure 6.

Enhancement of cytokine secretion after stimulation with NF nanoparticles is consistent with the amount of gp41-54Q-GHC released from polyanhydride nanoparticles. After stimulation with 125 μg/mL of NF or functionalized nanoparticles for 48 h, supernatants were collected and assayed for IL-6 and TNF-α. Data is represented as mean concentration of cytokines ± the SEM of three independent experiments performed in triplicate for antigen-loaded nanoparticles and two independent experiments in triplicate for blank nanoparticles. LPS was used as a positive control stimulant, and non-stimulated cells (NS) were used as a negative control. LPS control had the following MFI values: 50,000 for IL-6 and 25,000 for TNF-α. * and # represent statistical significance ($p \leq 0.05$) compared to the NS or NF groups, respectively. Cumulative mass of released gp41-54Q-GHC from NF and functionalized nanoparticles over 72 h. Results are expressed as the average of two independent experiments with duplicate samples in each.

Table 1

Characterization of functionalized polyanhydride nanoparticles

Total reaction time	Nanoparticle type	Particle diameter (nm)[a]	ζ potential (mV)[b]	Sugar density (μg/mg of particles)[c]	Sugar density (mmol/mol of polymer)[c]
0h	non-functionalized	184 ± 26	−20 ± 2.6		
2h (1/1)	linker	243 ± 38	23 ± 3.7		
2h (1/1)	di-mannose	295 ±34	25.4 ± 4.7	22.7 ± 1.2	282.9±15.0
4h (2/2)	di-mannose	285 ± 30	25.7 ± 3.1	20.8 ± 2.2	259.2±27.4
10h (5/5)	di-mannose	279 ± 37	24.6 ± 2.6	21.4 ± 1.8	266.7±22.4
18h (9/9)	di-mannose	272 ± 28	26.6 ± 3.0	17.1 ± 1.8	213.1±22.4

[a] Particle size data represent the mean ± standard deviation (SD) of dynamic light scattering data collected in two independent experiments.

[b] Zeta potential data represent the mean ± SD of three independent experiments.

[c] Sugar density data is presented as mean ± SD of two independent experiments.